

SCIENTIFIC REPORTS

OPEN

Radiation-induced magnetoresistance oscillations in monolayer and bilayer graphene

R. G. Mani, A. Kriisa  & R. Munasinghe

We examine the characteristics of the microwave/mm-wave/terahertz radiation-induced magnetoresistance oscillations in monolayer and bilayer graphene and report that the oscillation frequency of the radiation-induced magnetoresistance oscillations in the massless, linearly dispersed monolayer graphene system should depend strongly both on the Fermi energy, and the radiation frequency, unlike in the case of the massive, parabolic, GaAs/AlGaAs 2D electron system, where the radiation-induced magnetoresistance oscillation frequency depends mainly on the radiation frequency. This possible dependence of the magnetoresistance oscillation frequency on the Fermi level at a fixed radiation frequency also suggests a sensitivity to the gate voltage in gated graphene, which suggests an *in-situ* tunable photo-excitation response in monolayer graphene that could be useful for sensing applications. In sharp contrast to monolayer graphene, bilayer graphene is expected to show radiation-induced magnetoresistance oscillations more similar to the results observed in the GaAs/AlGaAs 2D system. Such expectations for the radiation-induced magnetoresistance oscillations are presented here to guide future experimental studies in both of these modern atomic layer material systems.

Carrier scattering gives rise to electrical resistance – a measure of frictional losses within semiconductor specimens¹. Under microwave/mm-wave/terahertz photoexcitation, high mobility 2D electron systems confined, for example, within GaAs/AlGaAs heterostructures exhibit large amplitude “1/4 cycle shifted” magnetoresistance oscillations with resistance maxima in the vicinity of $E = (j + 3/4)\hbar\omega_c$, resistance minima near $E = (j + 1/4)\hbar\omega_c$, and nodes in the resistance oscillations in the vicinity of the cyclotron resonance, and integral and half-integral cyclotron resonance harmonics, i.e., $E = j\hbar\omega_c$ and $E = (j + 1/2)\hbar\omega_c$. Here, E = energy, $\omega_c = eB/m^*$, e = electron charge, m^* = electron effective mass, \hbar = the reduced Planck constant, and B = the magnetic field. Most remarkably, at the lowest temperatures under modest photo-excitation, the deepest resistance minima saturate into zero-resistance states², about $B = 4/5B_f$ and $B = 4/9B_f$, of the characteristic field $B_f = 2\pi fm^*/e$, where f is the electromagnetic-wave frequency^{2–83}. That is, experiments suggest that the diagonal resistance can be switched off in the 2D electron system by photo-excitation in the presence of a small magnetic field. Such experimental reports have motivated the theoretical study of transport in photo-excited 2D semiconductor specimens^{57–83}. Large amplitude magnetoresistance oscillations under photoexcitation also imply strong electrical sensitivity to electromagnetic waves, which could potentially be applied towards the realization of microwave/mm-wave/terahertz photodetectors^{84–87}. Indeed, since the observations thus far have indicated $B_f = 2\pi fm^*/e$, the implication is that radiation frequency $f = eB_f/2\pi m^*$ can be determined from the characteristic field B_f of the magnetoresistance oscillations. The concurrent observed sensitivity to both the radiation-intensity and frequency has suggested the possibility of a tuned narrow band radiation sensor in the microwave/mm-wave/terahertz bands²⁵.

Above mentioned radiation-induced magnetoresistance oscillations have already served to characterize material systems such as GaAs/AlGaAs heterostructures^{2,3,5–7,9,11,13,15–17,19–55}, strained Si/SiGe⁸⁸, electrons on the surface of liquid Helium^{44,89}, and the oxide MgZnO/ZnO 2DES system⁹⁰ for scattering lifetimes, and effective masses. Thus, one expects that photo-excited magnetotransport studies of modern atomic layer 2D systems such as monolayer and bilayer graphene could potentially unveil new science and applications^{46,91–99}. However, the expectations for device response of these materials is not known and such phenomena have not been observed thus far in the graphene system. As a consequence, a question of interest is: what will be the oscillatory resistance response of modern atomic layered 2D materials such as, for example, graphene under electromagnetic wave excitation in a magnetic field? Below, we examine the expected characteristics for both the monolayer and bilayer graphene

Georgia State University, Department of Physics and Astronomy, Atlanta, GA, 30303, USA. Correspondence and requests for materials should be addressed to R.G.M. (email: mani.rg@gmail.com)

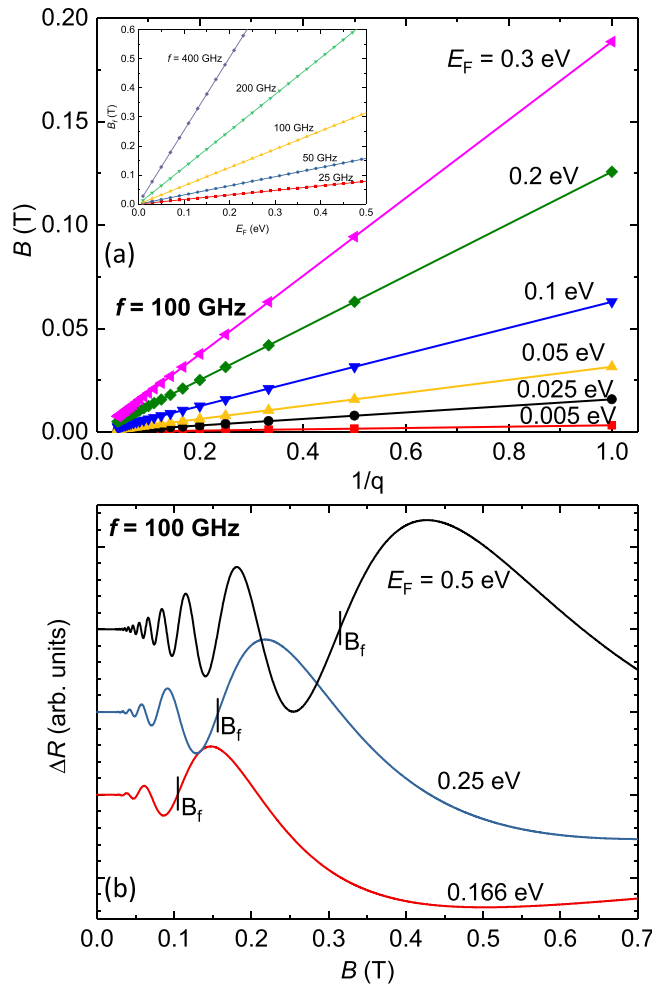


Figure 1. (a) For monolayer graphene, the magnetic field values, B , for nodes in the microwave induced magnetoresistance oscillations are plotted vs. the inverse node index, $1/q$, with $q = 1, 2, 3, \dots$, for different values of the Fermi energy, E_F , at a microwave frequency of $f = 100$ GHz. The inset shows the characteristic field or oscillation frequency B_f of the microwave induced magnetoresistance oscillations as a function of the Fermi energy, E_F , for radiation frequencies $f = 25, 50, 100, 200,$ and 400 GHz. (b) This figure illustrates the expected oscillatory magnetoresistance, ΔR , vs. B , in monolayer graphene under microwave photo-excitation at $f = 100$ GHz for three values of the Fermi energy, E_F . Note that the characteristic magnetic field, B_f , of the oscillatory magneto-resistance increases with E_F .

systems. As mentioned above, our results suggest a strong sensitivity of the response in monolayer graphene to both the Fermi energy and the radiation frequency. However, bilayer graphene is expected to show a more GaAs/AlGaAs like behavior, characteristic of parabolically dispersed systems. The results are summarized below.

It is well known that the Landau level dispersion for Dirac fermions in monolayer graphene is given by $E_N = \text{sgn}(N)(2\hbar eBN)^{1/2}v_F$ ^{97,98}. Here, N is the Landau level index, and v_F is the carrier velocity. Suppose that the Fermi level lies in the N th Landau level, $E_N = E_F$, and the electromagnetic radiation induces transitions from N th Landau level to the $N + q$ th Landau level^{57,59–61}, such that $E_{N+q} = E_F + hf$, where h is Planck's constant, and f is the radiation frequency. From studies of the GaAs/AlGaAs system², it is known that nodes in the radiation-induced magnetoresistance oscillations appear when the radiation energy spans such an integral number of Landau levels, i.e., $E_{N+q} - E_N = hf$, where q denotes the order of the node. Consider $E_N^2 = 2\hbar eBNv_F^2$, and note that

$$E_{N+q}^2 - E_N^2 = 2\hbar eBqv_F^2 \tag{1}$$

Apply the identity $E_{N+q}^2 - E_N^2 = (E_{N+q} - E_N)(E_{N+q} + E_N)$. Let $E_{N+q} - E_N = hf$ and $E_{N+q} + E_N = 2E_F + hf$. Then, by substituting into Eq. 1, we obtain

$$(2E_F + hf)hf = 2\hbar eBqv_F^2 \tag{2}$$

or

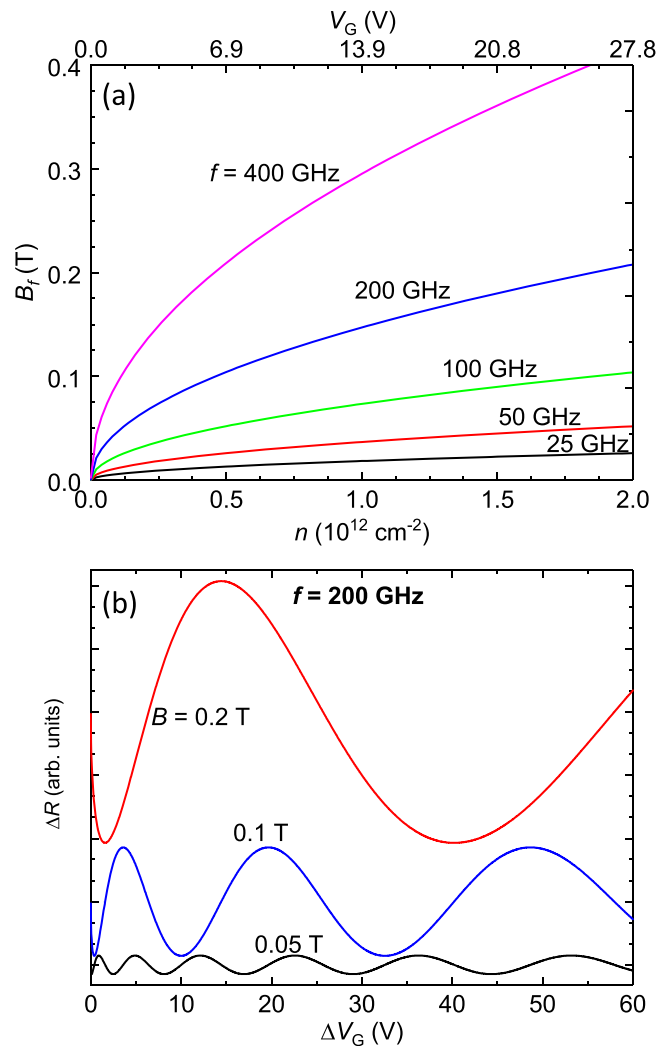


Figure 2. (a) The characteristic field or oscillation frequency B_f of radiation-induced magneto-resistance oscillations in monolayer graphene is plotted vs. the electron density, n , (bottom abscissa), and the gate voltage, ΔV_G , (top abscissa). B_f is proportional to $n^{1/2}$ and $\Delta V_G^{1/2}$. (b) This figure illustrates the expected oscillatory magneto-resistance, ΔR , vs. the gate voltage difference with respect to the neutrality voltage, ΔV_G , in monolayer graphene under microwave photo-excitation at $f = 200$ GHz for three values of the magnetic field, B . Here, since the extrema are periodic in $(\Delta V_G)^{1/2}$, they become further apart with increasing ΔV_G .

$$B = (1/q)(\pi f/e)(2E_F/v_F^2 + hf/v_F^2) \quad (3)$$

Thus, Eq. 3 describes the magnetic field values for the q 'th node of radiation-induced magnetoresistance oscillations in monolayer graphene and it suggests that such oscillations in monolayer graphene are also dependent upon value of the Fermi energy, E_F , unlike in the GaAs/AlGaAs system^{2,5,7,9,11,13,15,17,25,27,31,35,41}. In Fig. 1(a), we plot the nodal positions in magnetic field, B , vs. the inverse of integers, $1/q$, for several typical values of the Fermi energy in monolayer graphene. The figure shows a set of straight lines, which indicates that the expected magneto-resistance oscillations are periodic in B^{-1} , just as in the GaAs/AlGaAs system. The characteristic frequency or field, B_f , of the radiation-induced magnetoresistance oscillations that appears in the empirical formula for the oscillatory magnetoresistance lineshape $\Delta R \approx -\exp(-\lambda/B) \sin(2\pi B_f/B)$ ¹¹, is found from the slopes in Fig. 1(a) of B vs. $1/q$, which suggest increases of B_f with E_F , at a fixed radiation frequency, $f = 100$ GHz. The inset of Fig. 1(a) shows the variation of this characteristic frequency B_f of the radiation-induced magnetoresistance oscillation with E_F at several radiation frequencies, $f = 25, 50, 100, 200$ and 400 GHz. The inset conveys that B_f increases faster with E_F at larger radiation frequencies f . Note that B_f increases linearly with f over this range of f since $E_F \gg hf$, see eqn. 3. For $f = 100$ GHz, $hf = 4.125 \times 10^{-4}$ eV is much smaller than a small practical value for E_F such as $E_F = 5 \times 10^{-3}$ eV.

The expectations for the oscillatory resistance, $\Delta R \approx -\exp(-\lambda/B) \sin(2\pi B_f/B)$ ¹¹, in the monolayer graphene system are illustrated in Fig. 1(b), which exhibits ΔR vs. B at $E_F = 0.5, 0.25$, and 0.166 eV for photoexcitation at $f = 100$ GHz. Since the characteristic field B_f increases with E_F , and the parameters B, f, e , and v_F in Eq. 3 can be

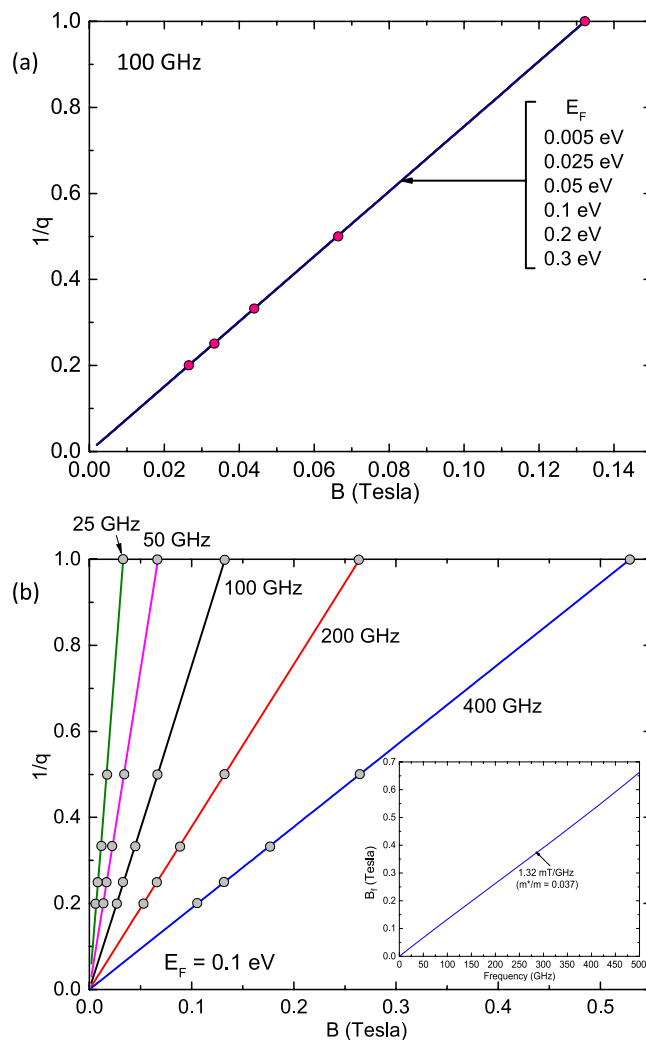


Figure 3. (a) For radiation-induced magneto-resistance oscillations in bilayer graphene, the inverse node index, $1/q$, for $q = 1, 2, 3, \dots$ is plotted vs the magnetic field, B , for various Fermi energies, E_F , at a radiation frequency, $f = 100$ GHz. (b) For radiation-induced magneto-resistance oscillations in bilayer graphene, the inverse node index, $1/q$, for $q = 1, 2, 3, \dots$ is plotted vs the magnetic field, B , for radiation frequencies $f = 25, 50, 100, 200,$ and 400 GHz. The plot implies that increasing the radiation frequency shifts the magneto-resistance oscillations to higher magnetic fields. The inset shows the magneto-resistance oscillation frequency, B_f , vs the radiation frequency, f . The plot shows that the slope of the line is 1.32 mT/GHz which corresponds to an effective mass ratio $m^*/m = 0.037$.

determined or are well known, the radiation-induced magneto-resistance oscillations in monolayer graphene can be utilized to accurately determine E_F .

From the experimental perspective, measurements can be carried out as a function of the magnetic field, B , or, as is more typical for graphene, vs. the gate voltage V_G . In monolayer graphene, the carrier density, n_q , varies as the square of the Fermi energy, i.e., $n_q = (4\pi/h^2)(E_F/v_F)^2$. Then,

$$B_f = (\pi f/e)(1/v_F^2)(2hv_F(n_q/4\pi)^{1/2} + hf) \quad (4)$$

Further, for graphene on top of 300 nm SiO_2 on doped Si the relation between the gate voltage and the carrier density is $n_q = \text{sgn}(\Delta V_G)\alpha|\Delta V_G|$ with $\alpha = 7.2 \times 10^{10} \text{ cm}^2/\text{V}^{97,98}$. Upon inserting these relations, we obtain from eqn. 4:

$$B_f = (\pi f/e)(1/v_F^2)(2hv_F(\alpha|\Delta V_G|/4\pi)^{1/2} + hf) \quad (5)$$

Figure 2(a) exhibits the dependence of the frequency or characteristic field B_f of the magneto-resistance oscillations vs. the electron density, i.e., $n_q = n$, and vs. the difference in the gate voltage with respect to the neutrality voltage, V_N , i.e., $\Delta V_G = V_G - V_N$. The square root dependence observed in Eqs 4 and 5 is manifested as a sub-linear variation of B_f with respect to these parameters at a fixed radiation frequency, f , i.e., $B_f \approx n^{1/2}$ and $B_f \approx \Delta V_G^{1/2}$.

Expectations for gate voltage dependence of the radiation-induced magnetoresistance oscillations in monolayer graphene following from Eq. 5 are exhibited in Fig. 2(b) for $f = 200$ GHz. The Fig. 2(b) shows that oscillations grow in amplitude with increasing magnetic field. Further, it is evident that the number of oscillations over a given span of gate voltage decreases with increasing B . Finally, the spacing between, say, successive oscillatory minima, increases with increasing ΔV_G because the magnetoresistance oscillations are actually periodic in $\Delta V_G^{1/2}$. From these numerical studies, it is clear that radiation-induced oscillations in monolayer graphene should be substantially different than the oscillations observed in the GaAs/AlGaAs system. The key differences are the dependence of the characteristic field or frequency B_f of the magnetoresistance oscillations upon the Fermi energy when $E_F \gg hf$ even at a fixed radiation frequency in monolayer graphene (Fig. 1(a)), the expected dependence of B_f on the gate voltage (Fig. 2), and the possibility of using such magnetoresistance oscillations to make a measurement of the Fermi energy in monolayer graphene.

Unlike in monolayer graphene, charge carriers in bilayer graphene are massive fermions as a consequence of the parabolic band structure. Bilayer graphene is a zero-gap system in the absence of a transverse electric field and it develops a bandgap under a transverse electric field^{97,98}. Consider the zero-gap case: The dispersion of carriers in zero-gap bilayer graphene under the influence of a magnetic field is given by $E_N = (N(N \pm 1))^{1/2} \omega_0 B$, where $\omega_0 = eh/m^*$, and $m^* = 0.037 m$ is the nominal effective mass of the carriers^{97,98}. Here, the + and - describe the response of the electron and the hole systems, and N can take on positive and negative integers for electrons and holes, respectively. To determine the expected response for the radiation-induced magnetoresistance oscillations in bilayer graphene with electrons, we suppose that at a magnetic field, B , the Fermi level lies in the N th Landau level, $E_N = E_F$, and the electromagnetic radiation induces transition from Landau level N to the $N + q$ Landau level so that $E_{N+q} = E_F + hf$. Further, assume that nodes in the radiation-induced magnetoresistance oscillations will appear when the radiation energy spans an integral number of Landau levels, i.e., $E_{N+q} - E_N = hf$, where q denotes the order of the node. To extract the characteristics for radiation-induced magnetoresistance oscillations in such a system, we examine:

$$E_{N+q}^2 - E_N^2 = (hf)(2E_F + hf) = \omega_0^2 B^2 q(q + 2N + 1) \quad (6)$$

By setting $E_N^2 = E_F^2 = N(N + 1)\omega_0^2 B^2$, we find $(N + 1/2) = ((E_F^2/\omega_0^2 B^2) + 1/4)^{1/2}$, to obtain

$$q = [hf(2E_F + hf)/(\omega_0^2 B^2) + (E_F^2/(\omega_0^2 B^2) + 1/4)]^{1/2} - (E_F^2/(\omega_0^2 B^2) + 1/4)^{1/2} \quad (7)$$

Equation 7 serves to determine the B -position of the nodes in the radiation-induced magnetoresistance oscillations as a function of the magnetic field for different values of the Fermi energy, E_F . Figure 3(a) presents $1/q$ vs. B for different values of the E_F at $f = 100$ GHz for bilayer graphene. The remarkable feature in this figure is the relative insensitivity of the results to the value of the Fermi energy for bilayer graphene, unlike in the case of monolayer graphene (see Fig. 1(a)). Thus, in this sense, bilayer graphene looks more similar to the GaAs/AlGaAs system.

The expected nodal B -positions, which are insensitive to E_F in bilayer graphene, are examined for different f in Fig. 3(b). Figure 3(b) shows that a given node, $q = 1, 2, 3, \dots$, shifts to higher B as f increases. Further, the frequency or characteristic field B_f of the radiation-induced magneto-resistance oscillations increases linearly with f in the limit where $E_F \gg hf$, as indicated in the inset of Fig. 3(b). Indeed, the characteristic field or frequency B_f -field should shift at the rate of 1.37 mT/GHz in bilayer graphene vis-à-vis the ≈ 2.35 mT/GHz shift observed in the GaAs/AlGaAs system. These calculations have assumed a fixed effective mass of $m^* = 0.037 m$ for bilayer graphene, while it is known that non-parabolicity could provide for variation in m^* with E_F ^{97,98}. Thus, studies of radiation induced magnetoresistance oscillations in bilayer graphene as a function of the carrier density could serve to characterize the non-parabolicity and determine the effective mass as a function of the energy.

In comparing the expectations for monolayer and bilayer graphene, the striking feature is the great dissimilarity in the E_F dependence of the radiation-induced oscillatory magnetoresistance characteristics. For monolayer graphene, the oscillations depend strongly on E_F and therefore also the ΔV_G . On the other hand, for bilayer graphene, there is a lack of sensitivity to E_F and therefore also on ΔV_G . This suggests that the characteristics of the observed magnetoresistance oscillations could also serve to differentiate between these two types of graphene.

References

- Ando, T., Fowler, A. B. & Stern, F. Electronic properties of two-dimensional systems. *Rev. Mod. Phys.* **54**, 437–672 (1982).
- Mani, R. G. *et al.* Zero-resistance states induced by electromagnetic wave excitation in GaAs/AlGaAs heterostructures. *Nature* **420**, 646–650 (2002).
- Zudov, M. A., Du, R. R., Pfeiffer, L. N. & West, K. W. Evidence for a new dissipationless effect in 2D electronic transport. *Phys. Rev. Lett.* **90**, 046807 (2003).
- Fitzgerald, R. Microwaves induce vanishing resistance in two dimensional electron systems. *Phys. Today* **56**(4), 24–27 (2003).
- Mani, R. G. *et al.* Demonstration of a 1/4 cycle phase shift in the radiation-induced oscillatory-magnetoresistance in GaAs/AlGaAs devices. *Phys. Rev. Lett.* **92**, 146801-1-4 (2004).
- Kovalev, A. E., Zvyagin, S. A., Bowers, C. R., Reno, J. L. & Simmons, J. A. Observation of a node in the quantum oscillations induced by microwave radiation. *Sol. St. Comm.* **130**, 379–381 (2004).
- Mani, R. G. *et al.* Radiation induced oscillatory Hall effect in high mobility GaAs/AlGaAs devices. *Phys. Rev. B* **69**, 161306-1-4 (2004).
- Dorozhkin, S. I. Giant magnetoresistance oscillations caused by cyclotron resonance harmonics. *JETP letters* **77**, 577–581 (2003).
- Mani, R. G. *et al.* Radiation induced zero-resistance states in GaAs/AlGaAs heterostructures: Voltage-current characteristics and intensity dependence at the resistance minima. *Phys. Rev. B* **70**, 155310-1-5 (2004).
- Zehnder, C., Wirthmann, A., Heyn, C. & Heitmann, D. Bolometric spin effect due to internal spin injection in a two dimensional electron system. *EuroPhys. Lett.*, textbf63, 576–582 (2003).
- Mani, R. G. *et al.* Radiation-induced oscillatory magnetoresistance as a sensitive probe of the zero-field spin splitting in high-mobility GaAs/AlGaAs devices. *Phys. Rev. B* **69**, 193304-1-4 (2004).

12. Studenikin, S. A., Potemski, M., Coleridge, P. T., Sachrajda, A. S. & Wasilewski, Z. R. Microwave radiation induced magneto-oscillation in the longitudinal and transverse resistance of a two dimensional electron gas. *Sol. St. Comm.* **129**, 341–345 (2004).
13. Mani, R. G. Zero-resistance states induced by electromagnetic-wave excitation in GaAs/AlGaAs heterostructures. *Physica E (Amsterdam)* **22**, 1–6 (2004).
14. Du, R. R., Zudov, M. A., Yang, C. L., Pfeiffer, L. N. & West, K. W. Dissipationless 2D electronic transport effect induced by microwaves. *Physica E (Amsterdam)* **22**, 7–12 (2004).
15. Mani, R. G. Radiation-induced zero-resistance states with resolved Landau levels. *Appl. Phys. Lett.* **85**, 4962–4964 (2004).
16. Simovic, B., Ellenberger, C., Ensslin, K. & Wegscheider, W. Density dependence of microwave induced magnetoresistance oscillations in a two-dimensional electron gas. *Phys. Rev. B* **71**, 233303-1-4 (2005).
17. Mani, R. G. Radiation-induced oscillatory magnetoresistance in a tilted magnetic field in GaAs/AlGaAs devices. *Phys. Rev. B* **72**, 075327-1-5 (2005).
18. Kukushkin, I. V. *et al.* New type of B-periodic magneto-oscillations in a two dimensional electron system induced by microwave irradiation. *Phys. Rev. Lett.* **92**, 236803 (2004).
19. Mani, R. G. Photo-excited zero-resistance states in quasi-two-dimensional GaAs/AlGaAs devices. *Sol. St. Comm.* **144**, 409–412 (2004).
20. Smet, J. H. *et al.* Circular-polarization-dependent study of the microwave photoconductivity in a two-dimensional electron system. *Phys. Rev. Lett.* **95**, 116804-1-4 (2005).
21. Mani, R. G. Spin characterization and control over the regime of the radiation-induced zero-resistance states. *IEEE Trans. Nanotechnol.* **4**, 27–34 (2005).
22. Mani, R. G. Radiation-induced decay of Shubnikov-de Haas oscillations in the regime of the radiation-induced zero-resistance states. *Appl. Phys. Lett.* **91**, 132103-1-3 (2007).
23. Wirthmann, A. *et al.* Far-infrared-induced magnetoresistance oscillations in GaAs/AlGaAs-based two-dimensional electron systems. *Phys. Rev. B* **76**, 195315-1-5 (2007).
24. Studenikin, S. A. *et al.* Frequency quenching of microwave-induced resistance oscillations in a high-mobility two-dimensional electron gas. *Phys. Rev. B* **76**, 165321-1-6 (2007).
25. Mani, R. G. Narrow-band radiation-sensing in the Terahertz and microwave bands using the radiation-induced magnetoresistance oscillations. *Appl. Phys. Lett.* **92**, 102107-1-3 (2008).
26. Wiedmann, S. *et al.* Interference oscillations of microwave photoresistance in double quantum wells. *Phys. Rev. B* **78**, 121301-1-4 (2008).
27. Mani, R. G., Johnson, W. B., Umansky, V., Narayanamurti, V. & Ploog, K. Phase study of oscillatory resistances in microwave irradiated and dark GaAs/AlGaAs devices: Indications of an unfamiliar class of integral quantum Hall effect. *Phys. Rev. B* **79**, 205320-1-10 (2009).
28. Chepelianskii, A. D. & Shepelyansky, D. L. Microwave stabilization of edge transport and zero-resistance states. *Phys. Rev. B* **80**, 241308-1-4 (2009).
29. Wiedmann, S. *et al.* Magnetoresistance oscillations in multilayer systems: Triple quantum wells. *Phys. Rev. B* **80**, 245306-1-9 (2009).
30. Konstantinov, D. & Kono, K. Photon-induced vanishing of magnetoconductance in 2D electrons on liquid helium. *Phys. Rev. Lett.* **105**, 226801-1-4 (2010).
31. Mani, R. G., Gerl, C., Schmult, S., Wegscheider, W. & Umansky, V. Nonlinear growth with the microwave intensity in the radiation-induced magnetoresistance oscillations. *Phys. Rev. B* **81**, 125320-1-6 (2010).
32. Wiedmann, S., Gusev, G. M., Raichev, O. E., Bakarov, A. K. & Portal, J. C. Thermally activated intersubband scattering and oscillating magnetoresistance in quantum wells. *Phys. Rev. B* **82**, 165333-1-8 (2010).
33. Wiedmann, S., Gusev, G. M., Raichev, O. E., Bakarov, A. K. & Portal, J. C. Microwave zero-resistance states in a bilayer electron system. *Phys. Rev. Lett.* **105**, 026804-1-4 (2010).
34. Ramanayaka, A. N., Mani, R. G. & Wegscheider, W. Microwave induced electron heating in the regime of the radiation-induced magnetoresistance oscillations. *Phys. Rev. B* **83**, 165303-1-5 (2011).
35. Mani, R. G., Ramanayaka, A. N. & Wegscheider, W. Observation of linear-polarization-sensitivity in the microwave-radiation-induced magnetoresistance oscillations. *Phys. Rev. B* **84**, 085308-1-4 (2011).
36. Ramanayaka, A. N., Mani, R. G., Inarrea, J. & Wegscheider, W. Effect of rotation of the polarization of linearly polarized microwaves on the radiation-induced magnetoresistance oscillations. *Phys. Rev. B* **85**, 205315-1-6 (2012).
37. Mani, R. G., Hankinson, J., Berger, C. & de Heer, W. A. Observation of resistively detected hole spin resonance and zero-field pseudo-spin splitting in graphene. *Nature Commun.* **3**, 996, <https://doi.org/10.1038/ncomms1986> (2012).
38. Konstantinov, D., Monarkha, Y. & Kono, K. Effect of coulomb interaction on microwave-induced magnetoconductivity oscillations of surface electrons on liquid helium. *Phys. Rev. Lett.* **111**, 266802-1-5 (2013).
39. Mani, R. G., Kriisa, A. & Wegscheider, W. Magneto-transport characteristics of a 2D electron system driven to negative magneto-conductivity by microwave photoexcitation. *Sci. Rep.* **3**, 3478, <https://doi.org/10.1038/srep03478> (2013).
40. Mani, R. G. *et al.* Terahertz photovoltaic detection of cyclotron resonance in the regime of the radiation-induced magnetoresistance oscillations. *Phys. Rev. B* **87**, 245308-1-8 (2013).
41. Mani, R. G., Kriisa, A. & Wegscheider, W. Size-dependent giant-magnetoresistance in millimeter scale GaAs/AlGaAs 2D electron devices. *Sci. Rep.* **3**, 2747, <https://doi.org/10.1038/02747> (2013).
42. Mani, R. G., von Klitzing, K. & Ploog, K. Magnetoresistance over the intermediate localization regime in GaAs/AlGaAs quantum wires. *Phys. Rev. B* **48**, 4571–4574 (1993).
43. Ye, T., Liu, H.-C., Wegscheider, W. & Mani, R. G. Combined study of microwave-power/linear polarization dependence of the microwave-radiation-induced magnetoresistance oscillations in GaAs/AlGaAs devices. *Phys. Rev. B* **89**, 155307-1-5 (2014).
44. Chepelianskii, A. D., Watanabe, N., Nasyedkin, K., Kono, K. & Konstantinov, D. An incompressible state of a photo-excited electron gas. *Nat. Comm.* **6**, 7210, <https://doi.org/10.1038/ncomms8210> (2015).
45. Ye, T., Liu, H.-C., Wang, Z., Wegscheider, W. & Mani, R. G. Comparative study of microwave radiation-induced magnetoresistive oscillations induced by circularly- and linearly- polarized photoexcitation. *Sci. Rep.* **5**, 14880, <https://doi.org/10.1038/srep14880> (2015).
46. Mani, R. G. Method for determining the residual electron- and hole- densities about the neutrality point over the gate-controlled n-p transition in graphene. *Appl. Phys. Lett.* **108**, 033507 (2016).
47. Herrmann, T. *et al.* Analog of microwave-induced resistance oscillations induced in GaAs heterostructures by terahertz radiation. *Phys. Rev. B* **94**, 081301-1-5 (2016).
48. Liu, H.-C., Samaraweera, R. L., Reichl, C., Wegscheider, W. & Mani, R. G. Study of the angular phase shift in the polarization angle dependence of the microwave induced magnetoresistance oscillations. *Phys. Rev. B* **94**, 245312-1-7 (2016).
49. Shi, Q. *et al.* Shubnikov de Haas oscillations in a two-dimensional electron gas under subterahertz radiation. *Phys. Rev. B* **92**, 081405(R) (2015).
50. Wang, Z., Samaraweera, R. L., Reichl, C., Wegscheider, W. & Mani, R. G. Tunable electron heating induced giant magnetoresistance in the high mobility GaAs/AlGaAs 2D electron system. *Sci. Rep.* **6**, 38516, <https://doi.org/10.1038/srep38516> (2016).
51. Samaraweera, R. L. *et al.* Mutual influence between current-induced giant magnetoresistance and radiation-induced magnetoresistance oscillations in the GaAs/AlGaAs 2DES. *Sci. Rep.* **7**, 5074, <https://doi.org/10.1038/s41598-017-05351-8> (2017).

52. Liu, H.-C., Reichl, C., Wegscheider, W. & Mani, R. G. B-periodic oscillations in the Hall resistance induced by a dc-current bias under combined microwave excitation and dc-current bias in the GaAs/AlGaAs 2D system. *Scientific Reports* **8**, 7878, <https://doi.org/10.1038/s41598-018-26009-z> (2018).
53. Samaraweera, R. L. *et al.* Coherent backscattering in the quasi-ballistic ultra-high mobility GaAs/AlGaAs 2DES. *Scientific Reports* **8**, 10061 (2018).
54. Munasinghe, C. R. *et al.* Electron heating induced by an ac-bias current in the regime of Shubnikov-de Haas oscillations in the high mobility GaAs/AlGaAs two-dimensional electron system. *J Phys Condens Matter* **30**, 31 (2018).
55. Nanayakkara, T. R. *et al.* Electron heating induced by microwave photoexcitation in the GaAs/AlGaAs two-dimensional electron system. *Phys. Rev. B* **98**, 035304 (2018).
56. Mani, R. G. & von Klitzing, K. Localization at high magnetic fields in GaAs/AlGaAs. *Phys. Rev. B* **46**, 9877 (1992).
57. Durst, A. C., Sachdev, S., Read, N. & Girvin, S. M. Radiation-induced magnetoresistance oscillations in a 2D electron gas. *Phys. Rev. Lett.* **91**, 086803-1-4 (2003).
58. Ryzhii, V. & Suris, R. Nonlinear effects in microwave photoconductivity of two-dimensional electron systems. *J. Phys.: Cond. Matt.* **15**, 6855-6869 (2003).
59. Shi, J. & Xie, X. C. Radiation-induced zero-resistance state and the photon-assisted transport. *Phys. Rev. Lett.* **91**, 086801 (2003).
60. Ryzhii, V. I. Absolute negative conductivity in two-dimensional electron systems associated with acoustic scattering stimulated by microwave radiation. *Phys. Rev. B* **68**, 165406 (2003).
61. Lei, X. L. & Liu, S. Y. Radiation-induced magnetoresistance oscillation in a two-dimensional electron gas in Faraday geometry. *Phys. Rev. Lett.* **91**, 226805 (2003).
62. Andreev, A. V., Aleiner, I. L. & Millis, A. J. Dynamical symmetry breaking as the origin of the zero-dc-resistance state in an ac-driven system. *Phys. Rev. Lett.* **91**, 056803-1-4 (2003).
63. Koulakov, A. A. & Raikh, M. E. Classical model for the negative dc conductivity of ac-driven two-dimensional electrons near the cyclotron resonance. *Phys. Rev. B* **68**, 115324-1-4 (2003).
64. Lei, X. L. & Liu, S. Y. Radiation-induced magnetoresistance oscillation in a two-dimensional electron gas in Faraday geometry. *Phys. Rev. Lett.* **91**, 226805-1-4 (2003).
65. Rivera, P. H. & Schulz, P. A. Radiation-induced zero-resistance states: Possible dressed electronic structure effects. *Phys. Rev. B* **70**, 075314-1-6 (2004).
66. Mikhailov, S. A. Microwave-induced magnetotransport phenomena in two-dimensional electron systems: Importance of electrodynamic effects. *Phys. Rev. B* **70**, 165311 (2004).
67. Dmitriev, I. A., Vavilov, M. G., Aleiner, I. L., Mirlin, A. D. & Polyakov, D. G. Theory of microwave-induced oscillations in the magnetoconductivity of a two-dimensional electron gas. *Phys. Rev. B* **71**, 115316-1-11 (2005).
68. Torres, M. & Kunold, A. Kubo formula for Floquet states and photoconductivity oscillations in a two-dimensional electron gas. *Phys. Rev. B* **71**, 115313-1-13 (2005).
69. Lei, X. L. & Liu, S. Y. Radiation-induced magnetotransport in high mobility two-dimensional systems: Role of electron heating. *Phys. Rev. B* **72**, 075345-1-10 (2005).
70. Inarrea, J. & Platero, G. Theoretical approach to microwave radiation-induced zero-resistance states in 2D electron systems. *Phys. Rev. Lett.* **94**, 016806-1-4 (2005).
71. Inarrea, J. & Platero, G. Temperature effects on microwave-induced resistivity oscillations and zero-resistance states in two-dimensional electron systems. *Phys. Rev. B* **72**, 193414-1-4 (2005).
72. Raichev, O. E. Magnetic oscillations of resistivity and absorption of radiation in quantum wells with two populated subbands. *Phys. Rev. B* **78**, 125304-1-14 (2008).
73. Inarrea, J. Effect of frequency and temperature on microwave-induced magnetoresistance oscillations in two-dimensional electron systems. *Appl. Phys. Lett.* **92**, 192113-1-3 (2008).
74. Dmitriev, I. A., Khodas, M., Mirlin, A. D., Polyakov, D. G. & Vavilov, M. G. Mechanisms of the microwave photoconductivity in two-dimensional electron systems with mixed disorder. *Phys. Rev. B* **80**, 165327-1-9 (2009).
75. Inarrea, J., Mani, R. G. & Wegscheider, W. Sublinear radiation power dependence of photoexcited resistance oscillations in two-dimensional electron systems. *Phys. Rev. B* **82**, 205321-1-5 (2010).
76. Mikhailov, S. A. Theory of microwave-induced zero-resistance states in two-dimensional electron systems. *Phys. Rev. B* **83**, 155303-1-12 (2011).
77. Inarrea, J. Influence of linearly polarized radiation on magnetoresistance in irradiated two-dimensional electron systems. *Appl. Phys. Lett.* **100**, 242103-1-3 (2012).
78. Lei X. L. & Liu, S. Y. Linear polarization dependence of microwave-induced magnetoresistance oscillations in high mobility two-dimensional systems. *Phys. Rev. B* **86**, 205303-1-5 (2012).
79. Inarrea, J. Linear polarization sensitivity of magnetotransport in irradiated two-dimensional electron systems. *J. Appl. Phys.* **113**, 183717-1-5 (2013).
80. Zhironov, O. V., Chepelianskii, A. D. & Shepelyansky, D. L. Towards a synchronization theory of microwave-induced zero-resistance states. *Phys. Rev. B* **88**, 035410-1-14 (2013).
81. Raichev, O. E. Theory of magnetothermoelectric phenomena in high-mobility two-dimensional electron systems under microwave irradiation. *Phys. Rev. B* **91**, 235307-1-16 (2015).
82. Beltukov, Y. M. & Dyakonov, M. I. Microwave-induced resistance oscillations as a classical memory effect. *Phys. Rev. Lett.* **116**, 176801-1-5 (2016).
83. Chang, C.-C., Chen, G.-Y. & Lin, L. Dressed photon induced resistance oscillation and zero-resistance in arrayed simple harmonic oscillators with no impurity. *Sci. Rep.* **6**, 37763, <https://doi.org/10.1038/srep37763> (2016).
84. Phillips, T. G. & Keene, J. S. *Astronomy. Proc. IEEE* **80**, 1662 (1992).
85. Hu, B. B. & Nuss, M. C. Imaging with terahertz waves. *Opt. Lett.* **20**, 1716 (1999).
86. Jacobsen, R. H., Mittleman, D. M. & Nuss, M. C. Chemical recognition of gases and gas mixtures with terahertz waves. *Opt. Lett.* **21**, 2011 (1996).
87. Tonouchi, M. Cutting-edge terahertz technology. *Nature Photonics* **1**, 97 (2007).
88. Zudov, M. A. *et al.* Observation of microwave-induced resistance oscillations in a high mobility two-dimensional hole gas in a strained Ge/SiGe quantum well. *Phys. Rev. B* **89**, 125401 (2014).
89. Yamashiro, R., Abdurakhimov, L. V., Badrutinov, A. O., Monarkha, Y. P. & Konstantinov, D. Photoconductivity response at cyclotron-resonance harmonics in a nondegenerate two-dimensional electron gas on liquid Helium. *Phys. Rev. Lett.* **115**, 256802 (2015).
90. Karcher, D. F. *et al.* Observation of microwave induced resistance and photovoltage oscillations in MgZnO/ZnO heterostructures. *Phys. Rev. B* **93**, 041410 (2016).
91. Novoselov, K. S. *et al.* Electric field effect in atomically thin carbon films. *Science* **306**, 666 (2004).
92. Berger, C. *et al.* Ultrathin epitaxial graphite: 2D electron gas properties and a route toward graphene-based nanoelectronics. *J. Phys. Chem. B* **108**, 19912 (2004).
93. Novoselov, K. S. *et al.* Two-dimensional gas of massless Dirac fermions in graphene. *Nature* **438**, 197 (2005).
94. Zhang, Y. B., Tan, Y. W., Stormer, H. L. & Kim, P. Experimental observation of the quantum Hall effect and Berry's phase in graphene. *Nature* **438**, 201 (2005).

95. Berger, C. *et al.* Electronic confinement and coherence in patterned epitaxial graphene. *Science* **312**, 1191 (2006).
96. Geim, A. K. & Novoselov, K. S. The rise of graphene. *Nature Mater.* **6**, 183 (2007).
97. Castro Neto, A. H., Guinea, F., Peres, N. M. R., Novoselov, K. S. & Geim, A. K. The electronic properties of graphene. *Rev. Mod. Phys.* **81**, 109 (2009).
98. Das Sarma, S., Adam, S., Hwang, E. H. & Rossi, E. Electronic transport in two-dimensional graphene. *Rev. Mod. Phys.* **83**, 407 (2011).
99. Witowski, A. M. *et al.* Quasiclassical cyclotron resonance of Dirac fermions in highly doped graphene. *Phys. Rev. B*, **82**, 165305-1-6 (2010).

Acknowledgements

The magnetotransport work is supported by the NSF under ECCS 1710302. Microwave, mm-wave, and terahertz work was supported by the Army Research Office under W911NF-14-2-0076 and W911NF-15-1-0433.

Author Contributions

Modeling by R.G.M., A.K. and R.M. Manuscript by R.G.M. and A.K.

Additional Information

Competing Interests: The authors declare no competing interests.

Publisher's note: Springer Nature remains neutral with regard to jurisdictional claims in published maps and institutional affiliations.



Open Access This article is licensed under a Creative Commons Attribution 4.0 International License, which permits use, sharing, adaptation, distribution and reproduction in any medium or format, as long as you give appropriate credit to the original author(s) and the source, provide a link to the Creative Commons license, and indicate if changes were made. The images or other third party material in this article are included in the article's Creative Commons license, unless indicated otherwise in a credit line to the material. If material is not included in the article's Creative Commons license and your intended use is not permitted by statutory regulation or exceeds the permitted use, you will need to obtain permission directly from the copyright holder. To view a copy of this license, visit <http://creativecommons.org/licenses/by/4.0/>.

© The Author(s) 2019